El-Sherbiny et al. Journal Of Nanostructure in Chemistry 2013, 3:8
http://www.jnanochem.com/content/3/1/8

Journal of Nanostructure in Chemistry
a SpringerOpen Journal

ORIGINAL Open Access

# Green synthesis of densely dispersed and stable silver nanoparticles using myrrh extract and evaluation of their antibacterial activity

Ibrahim M El-Sherbiny[1,2*], Ehab Salih[3] and Fikry M Reicha[3]

**Abstract**

In the present study, green synthesis of densely dispersed and stable silver nanoparticles (Ag NPs) using myrrh extract as green-reducing and stabilizing agent was investigated. The Ag NPs were synthesized by exposing a mixture of $AgNO_3$ and myrrh extract to UV irradiation for different time intervals. The effects of parameters such as concentration of $AgNO_3$ and reaction time onto the physicochemical characteristics of the developed Ag NPs were studied. Formation of the Ag NPs was noted upon changing the solution color from pale yellow into brown and was confirmed by the appearance of surface plasmon resonance peaks at about 445 nm. The resulting Ag NPs were characterized by UV-vis spectrophotometry, transmission electron microscopy, Fourier transform infrared spectroscopy, and X-ray diffraction. The developed NPs demonstrated a relatively high antibacterial activity against *Bacillus thuringiensis* and *Pseudomonas aeruginosa* bacteria as compared to that of myrrh extract. The antibacterial activity increased with increasing the Ag NP concentration.

**Keywords:** Myrrh, Green synthesis, Silver, Nanoparticles, Antibacterial activity

## Background

Nanotechnology comprises the science and technology at dimensions below 100 of nanometers. At this scale, the physicochemical characteristics of materials are significantly different from those found in larger scales and bulk materials due to the quantum effects [1].

Synthesis of metal nanoparticles (NPs) is an expanding research area due to the wide range of their applications in various fields such as medicine, electronics, and energy [2]. One of the most important classes of metal NPs is that made of noble metals such as gold (Au), silver (Ag), and platinum (Pt) [3]. Among the noble metal NPs, Ag NPs are perhaps the most widely recognized for their applications in photonics [4-6], micro-electronics [7,8], photocatalysis [9,10], and lithography [11,12]. The widespread use of Ag NPs in medicine, for instance, can be attributed to their potent antimicrobial activity against a wide range of pathogenic microorganisms [13].

The production of significant amounts of Ag NPs is achievable using various physical and chemical techniques including laser ablation [14], lithography [15], and the photochemical reduction [16]. However, synthesis techniques remain relatively expensive and occasionally involve the use of some hazardous moieties [17].

Biosynthesis of Ag NPs using microorganisms like bacteria [18], fungi [19], and yeast [20] has been investigated. However, exploration of the plant extracts as the potential nanofactories for the green synthesis of Ag NPs has a growing interest due to the major benefit of this synthesis technique in protecting the environment [21].

In this study, new series of stable densely dispersed Ag NPs were obtained using an entirely green synthesis approach. In this approach, the natural non-toxic ingredients extracted from the myrrh plant were used, instead of common hazardous chemicals, in combination with UV light irradiation to create the Ag NPs. Myrrh extract has been used as reducing and capping agent for the synthesis of NPs which could be advantageous over microbial synthesis as there is no need of the elaborated process of culturing and maintaining the cells.

* Correspondence: imelsherbiny@gmail.com
[1]Zewail University, Zewail City of Science and Technology, 6th October City, Giza 12588, Egypt
[2]Chemistry Department, Faculty of Science, Mansoura University, Mansoura ET-35516, Egypt
Full list of author information is available at the end of the article

Myrrh has been used for long time as a medicine and wound dressing, and has also been closely associated with the health and purification rituals of women. The medical potential of myrrh was first described in China in 600 AD during the Tang Dynasty, and it is still used to date in Chinese medicine to treat wounds, relieve painful swelling, and menstrual pain associated with blood stagnation. Myrrh consists of water-soluble gum, alcohol-soluble resins, and volatile oil [22]. The gum constituent contains polysaccharides and proteins, whereas the volatile oils are composed of steroids, sterols, and terpenes; the myrrh's characteristic odor is attributed to the presence of furanosesquiterpenes [22].

## Results and discussion

### Formation of the Ag NPs

The myrrh can be considered a potential source of hydrocarbons, and it consists of water-soluble gum, alcohol-soluble resins, and volatile oil [22]. The gum constituent contains various polysaccharides and proteins, whereas the volatile oil is composed of steroids, sterols, and terpenes [22]. Many of these compounds in the myrrh extract, especially the polysaccharides and saccharide moieties illustrated in Figure 1, are expected to be responsible for the partial reduction process of $AgNO_3$ into metallic Ag. During the synthesis process, the aqueous $Ag^+$ ions were exposed to the myrrh extract which initiated the reduction process of the $Ag^+$ ions in solution, leading to the formation of Ag hydrosol. Then, a complete reduction of the $Ag^+$ ions into atomic Ag then to Ag NPs was achieved through UV irradiation reduction of the reaction mixture for different time intervals from 10 to 120 min.

The formation of Ag NPs was observed upon the color change of the myrrh extract from transparent yellow into brown, as shown in Figure 2, due to the coherent oscillation of electrons at the surface of NPs, resulting in surface plasmon resonance (SPR) [23]. The color change into brown was noted within 10 min, and the color intensity increased significantly with increasing the $AgNO_3$ concentration at a fixed volume of myrrh extract. The UV-vis spectrophotometry was also used to confirm the formation of the Ag NPs as shown in Figure 3. From Figure 3a, the SPR band steadily increased in intensity with a prominent peak at about 480 nm at 1 mM concentration and then made a blue shift up to about 445 nm with increasing UV irradiation reduction time. The change of color and intensity of the SPR band with increasing irradiation time might be due to the variation in concentration, size, and shape of the resulting Ag NPs [24]. The peak that appeared at around 390 nm is likely to arise from the myrrh extract. Increasing the concentration of the Ag NP precursor (Ag $NO_3$) from 1 to 15 mM also led to the increasing intensity of the SPR band with a blue shift from 480 to about 450 nm (Figure 3b).

### FTIR spectroscopy

FTIR analysis was carried out in order to identify the possible reducing and stabilizing biomolecules in the myrrh extract. The FTIR spectra of myrrh extract before and after the development of Ag NPs are shown in Figure 4. Both spectra are very similar and showed bands around 1045, 1445, 1438, 1635, 2855, 2925, and 3449 $cm^{-1}$. The band around 1,025 to 1,200 $cm^{-1}$ corresponds to the C-O stretching, while the weak bands in the 1,340 to 1,450 $cm^{-1}$ range can be attributed to aliphatic $CH_2$ and $CH_3$ groups, $CH_2$ groups of aldehydes and ketones, and the bending modes of O-H bonds in alcohols, phenols, and carboxylic acids [25]. The band around 1,620 to 1,650 $cm^{-1}$ corresponds to aromatic rings, while the band that appeared around 2,920 to 2,930 $cm^{-1}$ corresponds to the asymmetric stretching of the C-H bonds. The strong broad band appearing at about 3,440 $cm^{-1}$ in both FTIR spectra can be assigned to the stretching vibrations of O-H groups in alcohols and phenols [25]. This band in particular confirms the presence of various O-H groups in the myrrh extract (Figure 1) which is expected to play a good role in the reduction process of $Ag^+$ ions into Ag then to Ag NPs. This band at 3,340 $cm^{-1}$ in the Ag NP spectrum has also showed a slight shift when compared to that of the myrrh extract, indicating the formation of Ag NPs.

### X-ray diffraction analysis

The X-ray diffraction pattern of the myrrh-Ag NPs developed after 60 min of UV irradiation of 6 mM $AgNO_3$ is illustrated in Figure 5. As apparent from the figure, there is a broad peak that appeared at $2\theta = 20°$ which

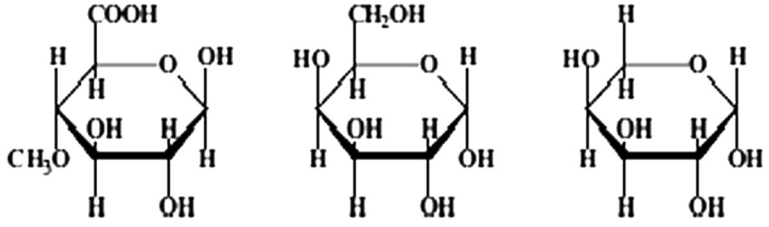


**Figure 1** Some saccharides in the myrrh extract (4-methyl D-glucuronic acid, D-galactose, and L-arabinose) [22].

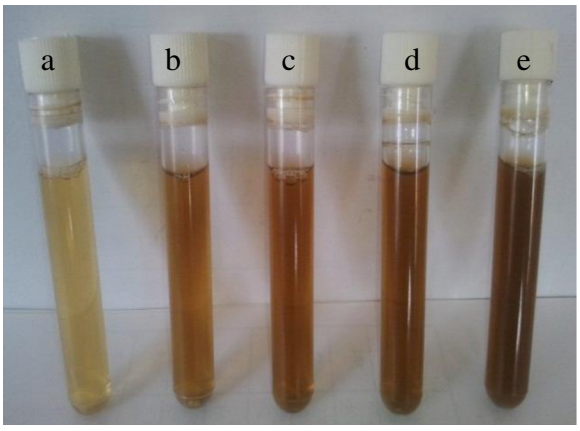


**Figure 2 The color change of the myrrh extract.** (**a**) Upon the formation of Ag NPs from different concentrations of $AgNO_3$: (**b**) 1 mM, (**c**) 4 mM, (**d**) 10 mM, and (**e**) 15 mM.

can be attributed to the amorphous phase of myrrh in addition to a number of Bragg reflections with $2\theta$ values of 38°, 44°, 64.6°, and 77°. These bands correspond to the (111), (200), (220), and (311) sets of lattice planes, which may be indexed as the bands for face centered cubic structures of Ag [26]. The XRD pattern, thus, clearly demonstrates that the Ag NPs synthesized by the present green method are crystalline in nature.

### Transmission electron microscopy

TEM has been employed to characterize the size, shape, and morphologies of the formed Ag NPs. The typical TEM micrographs and the corresponding particle size distribution of the myrrh-Ag NPs developed after 60 min of UV irradiation reduction of different concentrations of $AgNO_3$ are shown in Figure 6. As apparent from the figure, the obtained myrrh-Ag particles are in the nano range with uniform and spherical shapes. The myrrh-Ag NPs obtained using 1 mM of $AgNO_3$ followed by 60 min of UV irradiation (Figure 6a,c) showed average particle diameters from 40 to 100 nm. This particle size range was decreased to 10 to 50 nm by increasing the $AgNO_3$ concentration to 6 mM followed by 60 min of UV irradiation (Figure 6b,d). This result is in agreement with the blue shift observed in the UV-vis spectra of these samples (Figure 3). The TEM micrographs demonstrated also that the myrrh-Ag NPs are well and densely dispersed which indicates a good stabilization effect of the myrrh extract. The stability of the developed myrrh-Ag NPs was also confirmed through the absence of any visible changes for more than 6 months. Figure 6e shows the diffraction pattern of the developed NPs, which demonstrates the characteristic crystal planes of the elemental Ag.

### Antibacterial studies

The inhibition zone values were determined for the Ag NPs synthesized using myrrh extract tested against two types of bacteria, Gram positive (*B. thuringiensis*) and Gram negative (*P. aeruginosa*). The results of the inhibition zones were presented as average values (cm) as shown in Figure 7. The obtained data (Figure 7) demonstrate that all the investigated Ag NPs had high antibacterial activity against the Gram-positive (*B. thuringiensis*) bacteria and even much better antibacterial activity against the Gram-negative (*P. aeruginosa*) bacteria as compared to that of the control (myrrh extract). It is also apparent from Figure 7 that increasing the concentration of the Ag NPs has led to a significant increase in the antibacterial activity. This promising antibacterial activity may be related to the small size and the high surface area of the developed Ag NPs, which allow them

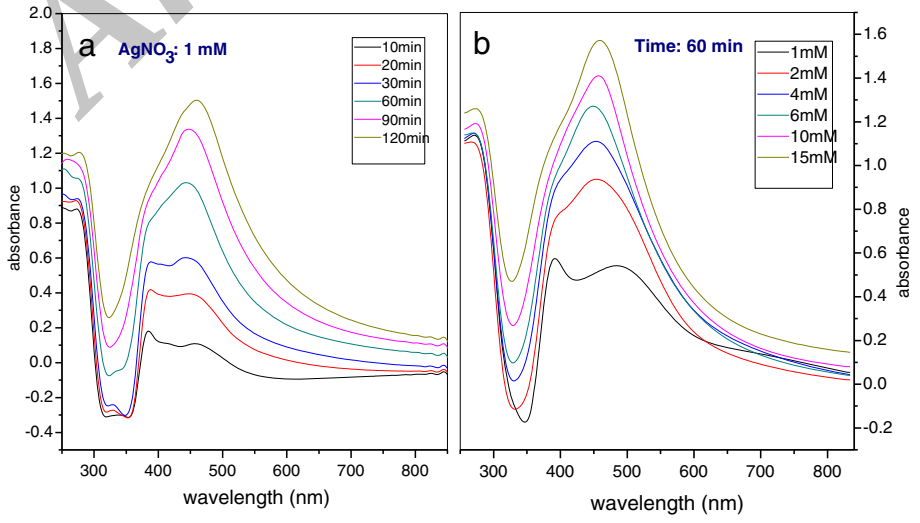


**Figure 3 UV-vis spectra.** UV-vis spectra of the formed Ag NPs recorded as a function of (**a**) time of UV irradiation and (**b**) $AgNO_3$ concentration.

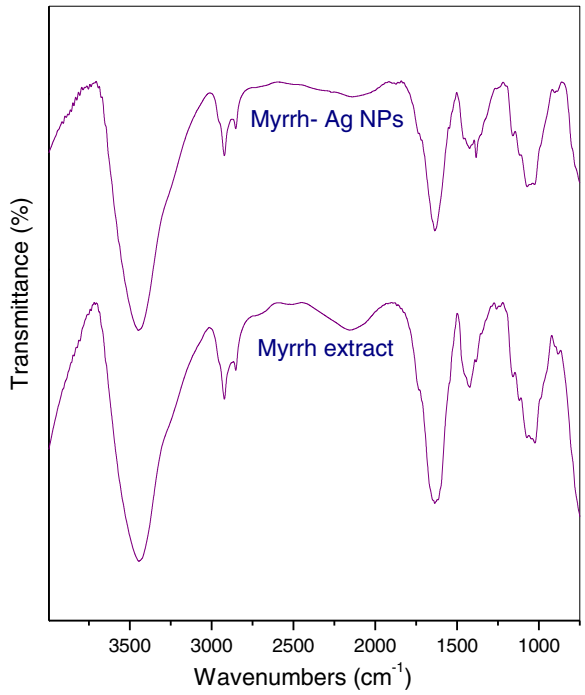


**Figure 4** FTIR spectra of the myrrh extract before and after the synthesis of Ag NPs.

to reach easily the nuclear content of bacteria [27,28]. Also, it has been reported that the pathogenic effect of the NPs can be attributed to their stability in the medium as colloids, which modulates the phosphotyrosine pattern of the pathogen proteins and consequently arrests their growth. Moreover, it was proposed that the variation in the growth inhibition of bacteria by NPs may be attributed to the presence of peptidoglycan, which has a strong negative complex structure [29]. This negative structure may participate in the sequestration of free $Ag^+$ ions. Therefore, Gram-positive bacteria may allow less Ag NPs to reach the cytoplasmic membrane than the Gram-negative bacteria, which tends to explain the founded higher antibacterial activity of the synthesized Ag NPs towards the Gram-negative (*P. aeruginosa*) bacteria than towards the Gram-positive one. These obtained preliminary results indicate a potential of the prepared myrrh-Ag NPs as antibacterial agents; however, further investigations are required to explore their bactericidal effects on other types of bacteria.

## Conclusion

The current study demonstrated that the Myrrh extract can be used as a green reducing and capping agent for the eco-friendly synthesis of Ag NPs. The developed Ag NPs showed good stability, and no visible changes were observed even after 6 months. The NPs also demonstrated high bactericidal activity against both *B. thuringiensis* and *P. aeruginosa* bacteria as compared to that of myrrh extract, and the antibacterial activity increased with increasing Ag NP concentration. In conclusion, this preliminary study revealed that the developed Ag NPs can be tailored and used, after more investigations, as potential antibacterial agents for various biological and biomedical applications.

## Methods

### Materials

Myrrh was purchased from a local market located at Mansoura, Egypt. Silver nitrate, ($AgNO_3$, AR grade, 99.5% purity) was obtained from Carl Roth GmbH & Co. KG (Schoemperlenstrasse, Karlsruhe, Germany). All of the other chemicals and solvents were of analytical grade and used as provided.

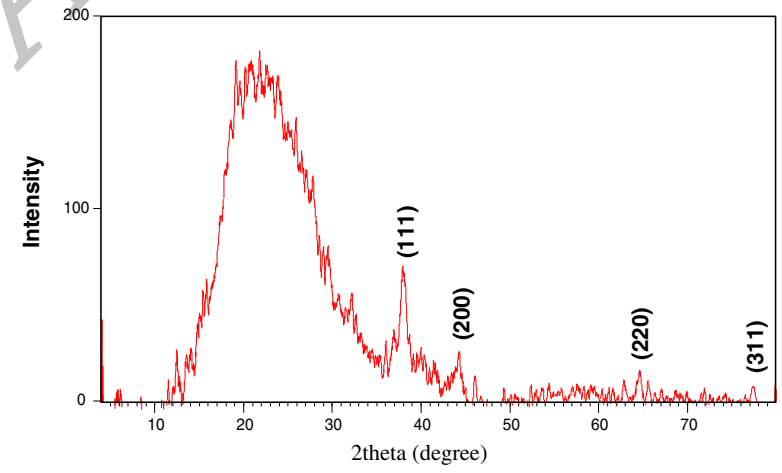


**Figure 5 XRD patterns.** XRD patterns of the Ag NPs developed after 60 min of UV irradiation of 6 mM $AgNO_3$.

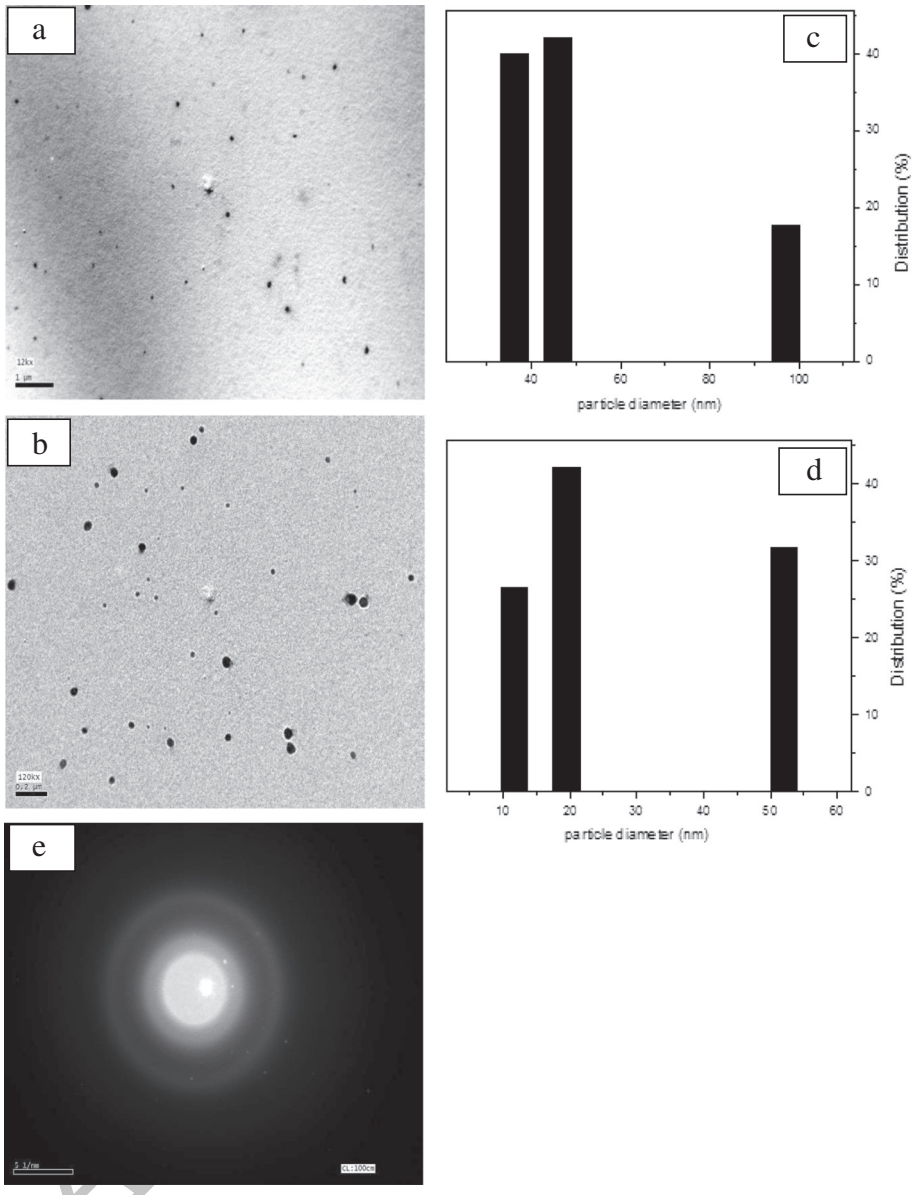


**Figure 6 TEM micrographs.** TEM micrographs of the Ag NPs developed in presence of the myrrh extract and 60 min of UV irradiation using different $AgNO_3$ concentrations. (**a**) 1 mM and (**b**) 6 mM. (**c**, **d**). The histograms of size distribution of the corresponding synthesized Ag NPs and (**e**) selected area of electron diffraction. The scale bars are (**a**) 1 μm, (**b**) 0.2 μm, and (**e**) μm.

### Preparation of myrrh extract

Myrrh parts were collected and washed thoroughly with distilled water and grinded into fine pieces. About 10 g of thoroughly washed finally grinded myrrh was weighted and transferred into a 300-ml Erlenmeyer flask containing 200-ml deionized water, mixed well and heated for 7 h in water bath at 80°C. The resulting solution was centrifuged at 4,000 rpm for 15 min and then filtered using Whatman number 1 filter paper, and the filtrate was stored at 4°C for further use.

### Synthesis of Ag NPs

Aqueous $AgNO_3$ solution (6 mM) was prepared and used for the synthesis of Ag NPs. Typically, 15 ml of myrrh aqueous extract was mixed with 60 ml of the $AgNO_3$ solution, and the resulting mixture was then irradiated by UV light (Philips UV lamp, 36 W; Koninklijke Philips Electronics N.V., Amsterdam, Netherlands) for different time intervals from 10 to 120 min. For studying the effect of $AgNO_3$ concentration, 5 ml of myrrh extract was added to 20 ml of different concentrations of the aqueous $AgNO_3$ solution

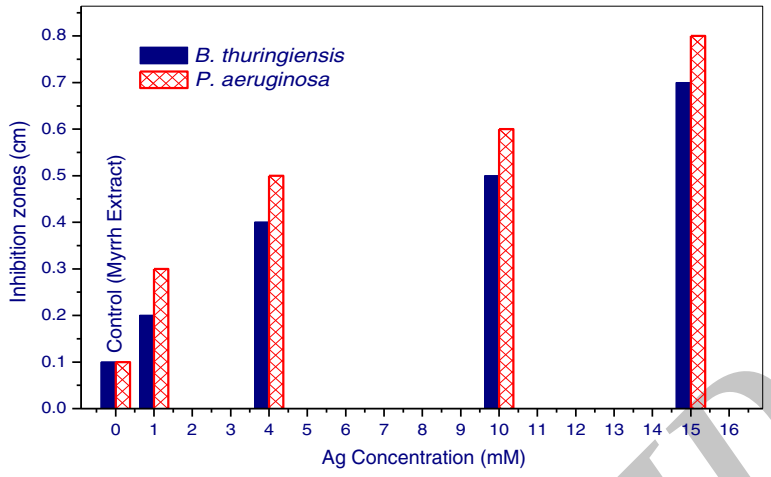


**Figure 7** The bacterial inhibition zones of the developed myrrh-Ag NPs of different $AgNO_3$ concentrations.

(1 to 15 mM) followed by UV irradiation reduction of the mixture for 60 min.

### Analysis of Ag NPs

The reduction of pure $Ag^+$ ions was monitored by measuring the UV-vis spectrum of the reaction medium at different time intervals. The UV-visible spectra of the formed Ag NPs were recorded in the range of 200 to 800 nm using ATI Unicom UV-vis spectrophotometer (UNICOM Systems, Inc., England) with the aid of ATI Unicom UV-vis. vision software V 3.20. The analysis was performed at room temperature using quartz cuvettes (1-cm optical path), and the blank was the corresponding myrrh aqueous solution. Fourier transform infrared spectroscopy (FTIR) measurements were carried out to identify the possible biomolecules in the aqueous extract of myrrh, which are responsible for the reduction of the $Ag^+$ ions and capping of the resulting Ag NPs. The sample was dried and grinded with KBr pellets and analyzed on Mattson 5000 FTIR spectrometer (Mattson Instruments, Inc., Wl, USA) in the range of 400 to 4,000 $cm^{-1}$ at a resolution of 8 $cm^{-1}$ at 25°C. The size and morphology of the synthesized Ag NPs were investigated by transmission electron microscopy (TEM; JEOL TEM-1230, JEOL Ltd., Tokyo, Japan) attached to a CCD camera at an accelerating voltage of 120 kV. The samples were prepared by placing few drops of the Ag NP suspension on carbon-coated copper grids, followed by allowing the solvent to slowly evaporate before recording the TEM images. The X-ray diffraction patterns of the Ag NP samples were recorded using Philips PW 1390 X-ray diffractometer (Netherland). The X-ray diffraction was provided with a beam monochromator and Cu K$\alpha$ radiation at $\lambda$ = 1.5406 Å. The applied voltage was 40 kV, and the current intensity was 40 mA sec. The $2\theta$ angles were recorded in the range of 40° to 60°.

### Assessment of the antibacterial activity

The antibacterial activity of myrrh aqueous extract and the Ag NPs developed at different $AgNO_3$ concentrations (1, 4, 10, and 15 mM) was evaluated against two types of bacteria, *Bacillus thuringiensis* and *Pseudomonas aeruginosa*, isolated from patients in Mansoura University Hospital, Mansoura, Egypt. The antibacterial assessment was performed using the nutrient agar diffusion method and measuring the inhibition zones (cm). In brief, sterile paper discs (6 mm) were impregnated overnight in the sample solutions and then left to dry for 24 h at 37°C in sterile conditions. The bacterial suspensions were obtained by making a saline suspension of isolated colonies selected from 18 to 24 h of nutrient agar plating. The suspensions were then adjusted to match the tube of 0.5 McFarland turbidity standards using spectrophotometry at $\lambda$ = 600 nm, which equals 1.5.108 colony-forming units per milliliter. The surface of the nutrient agar was completely inoculated using a sterile swab, which was steeped in the prepared bacterial suspension. Then, the impregnated discs were placed on the inoculated agar and incubated at 37°C for 24 h. After incubation, the diameters of the growth inhibition zones were determined.

#### Competing interests

The authors declare that they have no competing interests.

#### Authors' contributions

IME participated in the idea of the study, the design of the study, interpretation of the results, and writing the manuscript for publication. ES performed the green synthesis and the physicochemical characterization of the myrrh-Ag nanoparticles and early drafted the manuscript. FMR suggested the myrrh for the green synthesis of the Ag nanoparticles, conceived of the study, and participated in its coordination. All authors read and approved the final manuscript.

#### Authors' information

IME achieved the following in his academic years: B.Sc. and M.Sc. in Polymer Chemistry, Mansoura University, Egypt; Ph.D. in Drug Delivery from IFS,

Massey University, New Zealand; Postdoctoral Fellow from the College of Pharmacy, University of New Mexico, USA; and Postdoctoral Associate from the College of Pharmacy, University of Texas, Texas, USA. He is an Associate Professor from the Zewail University of Science and Technology, Egypt and an Associate Professor from Mansoura University, Egypt. He is a Research Assistant Professor in Pharmaceutics, Texas University at Austin, USA, and a Fellow of BMES, AAPS and NZ Institute of Chemistry. His research area interests cover smart nano-biomaterials, controlled drug delivery, wastewater treatment, tissue engineering, and gene therapy. ES obtained his BS in Physics from the Faculty of Science, Mansoura University, Egypt, with a graduation project on Fractional calculus. He earned his MSc in Physics with the thesis entitled 'Green synthesis of metal nanoparticles in plant extracts and evaluation of their physicochemical and biological characteristics', from the Faculty of Science, Mansoura University, Egypt. His research area interests include nanomaterials and biomaterials. FMR earned his BSc in Physics & Chemistry from the Faculty of Science, Alexandria University, Egypt. He is an MSc degree holder of Chemistry and Physics. He obtained his PhD in Thin Films from Magaryans. He was a Professor of Experimental Solid State Physics. He is the Head of Advanced Biomaterials Laboratory, Physics Department, Mansoura University. His research area covers nano-biotechnology, electrochemical polymerization and complexation, biomaterials, tissue engineering, AC-dielectric studies, and crystal science.

**Author details**
[1]Zewail University, Zewail City of Science and Technology, 6th October City, Giza 12588, Egypt. [2]Chemistry Department, Faculty of Science, Mansoura University, Mansoura ET-35516, Egypt. [3]Biological Advanced Materials, Physics Department, Faculty of Science, Mansoura University, Mansoura ET-35516, Egypt.

Received: 7 March 2013 Accepted: 30 March 2013
Published: 8 April 2013

**References**

1. Matos, RA, Cordeiro, TS, Samad, RE, Vieira Jr, ND, Courrol, LC: Green synthesis of stable silver nanoparticles using Euphorbia milii latex. Colloid Surface A **389**, 134–137 (2011)
2. Saxena, A, Tripathi, RM, Zafar, F, Singh, P: Green synthesis of silver nanoparticles using aqueous solution of Ficus benghalensis leaf extract and characterization of their antibacterial activity. Mater. Lett. **67**, 91–94 (2012)
3. Kaviya, S, Santhanalakshmi, J, Viswanathan, B, Muthumary, J, Srinivasan, K: Biosynthesis of silver nanoparticles using *Citrus sinensis* peel extract and its antibacterial activity. Spectrochim Acta A **79**, 594–598 (2011)
4. Inacio, PL, Barreto, BJ, Horowitz, F, Correia, RRB, Pereira, MB: Silver migration at the surface of ion-exchange waveguides: a plasmonic template. Opt Mater Express **3**, 390–399 (2013)
5. Hosel, M, Krebs, FC: Large-scale roll-to-roll photonic sintering of flexo printed silver nanoparticle electrodes. J. Mater. Chem. **22**, 15683–15688 (2012)
6. Gould, IR, Lenhard, JR, Muenter, AA, Godleski, SA, Farid, S: Two-electron sensitization: a new concept for silver halide photography. J. Am. Chem. Soc. **122**, 11934–11943 (2000)
7. Reddy, VR, Currao, A, Calzaferri, G: Gold and silver metal nanoparticle-modified AgCl photocatalyst for water oxidation to $O_2$. J. Phys. Conf. Ser. **61**, 960–965 (2007)
8. Deheer, WA: The physics of simple metal clusters: experimental aspects and simple models. Rev. Mod. Phys. **65**, 611–676 (1993)
9. Bawendi, MG, Steigerwald, ML, Brus, LE: The quantum mechanics of larger semiconductor clusters ("Quantum Dots"). Annu. Rev. Phys. Chem. **41**, 477–496 (1990)
10. Bar, H, Bhui, DK, Sahoo, GP, Sarkar, P, Pyne, S, Misra, A: Green synthesis of silver nanoparticles using seed extract of Jatropha curcas. Colloid Surface A **348**, 212–216 (2009)
11. Xia, Y, Rogers, JA, Paul, KE, Whitesides, GM: Unconventional methods for fabricating and patterning nanostructures. Chem. Rev. **99**, 1823–1848 (1999)
12. Shipway, AN, Lahav, M, Willner, I: Nanostructured gold colloid electrodes. Adv. Mater. **12**, 993–998 (2000)
13. Klaine, SJ, Alvarez, PJ, Batley, GE, Fernandes, TF, Handy, RD, Lyon, DY: Nanomaterials in the environment: behavior, fate, bioavailability and effects. Environ. Toxicol. Chem. **27**, 1825–1851 (2008)
14. Tsuji, T, Kakita, T, Tsuji, M: Preparation of nano-size particles of silver with femtosecond laser ablation in water. Appl. Surf. Sci. **206**, 314–320 (2003)
15. Jensen, TR, Malinsky, MD, Haynes, CL, Duyne, RPV: Nanosphere lithography: tunable localized surface plasmon resonance spectra of silver nanoparticles. J. Phys. Chem. B **104**, 10549–10556 (2000)
16. Lu, HW, Liu, SH, Wang, XL, Qian, XF, Yin, J, Zhu, ZK: Silver nanocrystals by hyperbranched polyurethane-assisted photochemical reduction of $Ag^+$. Mat Chem Phys **81**, 104–107 (2003)
17. Lukman, AI, Gong, B, Marjo, CE, Roessner, U, Harris, AT: Facile synthesis, stabilization, and anti-bacterial performance of discrete Ag nanoparticles using Medicago sativa seed exudates. J Colloid Interf Sci **353**, 433–444 (2011)
18. Saifuddin, N, Wong, CW, Nur Yasumira, AA: Rapid biosynthesis of silver nanoparticles using culture supernatant of bacteria with microwave irradiation. Eur. J. Chem. **6**, 61–70 (2009)
19. Duran, N, Marcato, PD, De Souza, GIH, Alves, OL, Esposito, E: Mechanistic aspects of biosynthesis of silver nanoparticles by several Fusarium oxysporum strains. J. Biomed. Nanotechnol. **3**, 1–8 (2009)
20. Kowshik, M, Ashtaputre, S, Kharrazi, S, Vogel, W, Urban, J, Kulkarni, SK, Paknikar, KM: Extracellular synthesis of silver nanoparticles by a silver-tolerant yeast strain MKY3. Nanotechnology **14**, 95–100 (2003)
21. Jacob, SJP, Finub, JS, Narayanan, A: Synthesis of silver nanoparticles using Piper longum leaf extracts and its cytotoxic activity against Hep-2 cell line. Colloid Surfaces B **91**, 212–214 (2012)
22. Hanusa, LO, Rezankab, T, Dembitskya, VM, Moussaieff, A: Myrrh—commiphora chemistry. Biomed Pap **149**, 3–28 (2005)
23. Narayanan, KB, Sakthivel, N: Extracellular synthesis of silver nanoparticles using the leaf extract of Coleus amboinicus Lour. Mater. Res. Bull **46**, 1708–1713 (2011)
24. Rani, PU, Rajasekharreddy, P: Green synthesis of silver-protein (core–shell) nanoparticles using Piper betle L. leaf extract and its ecotoxicological studies on Daphnia magna. Colloid Surface A **389**, 188–194 (2011)
25. Yilmaz, M, Turkdemir, H, Kilic, MA, Bayram, E, Cicek, A, Mete, A, Ulug, B: Biosynthesis of silver nanoparticles using leaves of Stevia rebaudiana. Mater. Chem. Phys. **130**, 1195–1202 (2011)
26. Sathishkumar, M, Sneha, K, Won, SW, Cho, CW, Kim, S, Yun, YS: Cinnamon zeylanicum bark extract and powder mediated green synthesis of nano-crystalline silver particles and its bactericidal activity. Colloid Surfaces B **73**, 332–338 (2009)
27. Reicha, FM, Sarhan, A, Abdel-Hamid, MI, El-Sherbiny, IM: Preparation of silver nanoparticles in the presence of chitosan by electrochemical method. Carbohydr. Polym. **89**, 236–244 (2012)
28. Lok, CN, Ho, CM, Chen, R, He, QY, Yu, WY, Sun, H, Tam, PK, Chiu, JF, Che, CM: Proteomic analysis of the mode of antibacterial action of silver nanoparticles. J. Proteome Res. **5**, 916–924 (2006)
29. Ahmad, N, Sharma, S, Singh, VN, Shamsi, SF, Fatma, A, Mehta, BR: Biosynthesis of silver nanoparticles from Desmodium trifolium: a novel approach towards weed utilization. Biotech Res Int **8**, 1–8 (2011)

doi:10.1186/2193-8865-3-8
**Cite this article as:** El-Sherbiny *et al.*: **Green synthesis of densely dispersed and stable silver nanoparticles using myrrh extract and evaluation of their antibacterial activity.** *Journal Of Nanostructure in Chemistry* 2013 **3**:8.